Environment International 173 (2023) 107783

Contents lists available at ScienceDirect

Environment International

journal homepage: www.elsevier.com/locate/envint

Full length article

Associations between short-term temperature exposure and kidney-related conditions in New York State: The influence of temperature metrics across four dimensions

Lingzhi Chu [a,b,*], Kai Chen [a,b], Susan Crowley [c,d], Robert Dubrow [a,b]

[a] Department of Environmental Health Sciences, Yale School of Public Health, 60 College Street, New Haven, CT 06520-8034, USA
[b] Yale Center on Climate Change and Health, Yale School of Public Health, 60 College Street, New Haven, CT 06520-8034, USA
[c] Department of Medicine (Nephrology), Yale University School of Medicine, New Haven, CT 06520, USA
[d] Veterans Administration Health Care System of Connecticut, West Haven, CT 06516, USA

ARTICLE INFO

Handling Editor: Hanna Boogaard

Keywords:
Kidney disease
Temperature
Heat exposure
Climate change
Spatial resolution
Wet-bulb globe temperature
Meteorological variables

ABSTRACT

Background: Evidence describing the relationship between short-term temperature exposure and kidney-related conditions is insufficient. It remains unclear how temperature specification affects estimation of these associations. This study aimed to assess associations between short-term temperature exposure and seven kidney-related conditions and to evaluate the influence of temperature specification.

Methods: We obtained data on hospital encounters in New York State (2007–2016). We assessed associations with a case-crossover design using conditional logistic regression with distributed lag non-linear models. We compared model performance (i.e., AIC) and association curves using 1) five temperature spatial resolutions; 2) temperature on an absolute versus relative scale; 3) seven temperature metrics incorporating humidity, wind speed, and/or solar radiation; and 4) five intraday temperature measures (e.g., daily minimum and daytime mean).

Results: We included 1,209,934 unplanned adult encounters. Temperature metric and intraday measure had considerably greater influence than spatial resolution and temperature scale. For outcomes not associated with temperature exposure, almost all metrics or intraday measures showed good model performance; for outcomes associated with temperature, there were meaningful differences in performance across metrics or intraday measures. For parsimony, we modelled daytime mean outdoor wet-bulb globe temperature, which showed good performance for all outcomes. At lag 0–6 days, we observed increased risk at the 95th percentile of temperature versus the minimum morbidity temperature for acute kidney failure (odds ratio [OR] = 1.36, 95% confidence interval [CI]: 1.09, 1.69), urolithiasis (OR = 1.41, 95% CI: 1.16, 1.70), dysnatremia (OR = 1.26, 95% CI: 1.01, 1.59), and volume depletion (OR = 1.88, 95% CI: 1.41, 2.51), but not for glomerular diseases, renal tubulo-interstitial diseases, and chronic kidney disease.

Conclusions: High-temperature exposure over one week is a risk factor for acute kidney failure, urolithiasis, dysnatremia, and volume depletion. The differential model performance across temperature metrics and intraday measures indicates the importance of careful selection of exposure metrics when estimating temperature-related health burden.

1. Introduction

Kidney disease is a globally prevalent non-communicable disease. In the U.S. alone, in 2021, 37 million adults were living with chronic kidney disease (CKD), which is a risk factor for kidney failure, cardiovascular disease, and premature death (US Department of Health Human Services CDC, 2021). CKD may arise from repeated episodes of acute kidney injury (which may result in acute kidney failure [AKF]) and/or from complications related to urolithiasis (Yang et al., 2010; Singh et al., 2021). Higher ambient temperature could lead to acute

* Corresponding author at: Department of Environmental Health Sciences, and Yale Center on Climate Change and Health, Yale School of Public Health, 60 College Street, New Haven, CT, 06520-8034, USA.
E-mail address: lingzhi.chu@yale.edu (L. Chu).

https://doi.org/10.1016/j.envint.2023.107783
Received 17 October 2022; Received in revised form 12 December 2022; Accepted 26 January 2023
Available online 30 January 2023

kidney injury through mechanisms including dehydration and elevated core temperature (Jimenez et al., 2014; García-Arroyo et al., 2016; Roncal-Jimenez et al., 2016; García-Arroyo et al., 2017; Holt and Moore, 2001). In the era of climate change, the contribution of ambient temperature to acute and chronic kidney dysfunction is a topic of increasing interest.

Existing epidemiologic evidence supports high ambient temperature exposure as an acute risk factor for AKF (Chen et al., 2017; McTavish et al., 2018) and urolithiasis (Tasian et al., 2014; Ordon et al., 2016). However, much research has focused on exposure to high temperatures rather than exposures across the entire temperature range, and on AKF and urolithiasis, with few studies on other kidney disease subtypes. Furthermore, the estimation of associations between ambient temperature and kidney disease outcomes could be influenced by the specification of the temperature variable in a number of dimensions including: (1) spatial resolution; (2) absolute (i.e., degrees Celsius) versus relative (i.e., quantiles) temperature; (3) incorporation of other meteorological variables (i.e., humidity, wind speed, solar radiation) into the measurement (e.g., heat index, wet-bulb globe temperature [WBGT]); and (4) intraday measures (e.g., daily mean, daily minimum, nighttime mean).

In epidemiologic studies, spatial resolution of temperature exposure is usually on the weather-monitor- (Chen et al., 2017; Heidari et al., 2016), city- (Mendez-Lazaro et al., 2018), or county-level (Bobb et al., 2014), depending on the data source. With recent advances in the application of satellite-derived land surface temperature and machine learning approaches, spatiotemporally highly-resolved estimates of ambient temperature exposures (e.g., 1 km $\times$ 1 km resolution in the spatial scale) are emerging (Jin et al., 2021; Kloog et al., 2014). With residential address at the centroid of the geographic area used to estimate temperature exposure for an individual, coarser spatial resolution may not represent an accurate exposure estimate for people who spend most of their time near home, whereas finer resolution may not represent an accurate estimate for people who spend most of their time away from home. To address this methodologic issue, studies on the relationship between ambient temperature exposure and kidney disease risk across different spatial resolutions within the same population using the same temperature data source are needed.

Few studies have compared use of absolute temperature (i.e., degrees Celsius) versus relative temperature (i.e., quantiles) in assessing the relationship between temperature exposure and kidney disease risk. While use of the Celsius scale is intuitive, the interpretation of its use could be complicated if the relationship between absolute temperature and kidney disease risk were heterogeneous across climate zones included in an epidemiologic study due to physiological, behavioral, and/or built environment adaptation. In this situation, the relationship could not be summarized succinctly, and climate-zone-specific estimates would need to be presented. Alternatively, use of a relative scale might result in homogeneity of the relationship across climate zones (e.g., the relative risk for the 95th percentile of temperature compared to the 50th percentile of temperature might be the same across climate zones, whereas the relative risk for 30 °C compared to 20 °C might differ across climate zones), allowing for parsimonious presentation of results.

Most previous studies of the relationship between temperature and kidney disease risk have used simple ambient temperature (i.e., dry-bulb temperature) as the measure of exposure (Liu et al., 2021), although some have incorporated humidity through use of a common temperature-humidity index such as humidex (McTavish et al., 2018). However, few studies have assessed more complex metrics of heat stress that incorporate wind speed and/or solar radiation (e.g., WBGT), which, like humidity, affect "the felt temperature." Furthermore, most previous epidemiologic studies used daily mean temperature as the intraday temperature measure, although some studies have demonstrated that different intraday temperature measures lead to different association estimates (Borg et al., 2017; Goldie et al., 2018), implying different underlying physiological pathways. For example, if the relationship between temperature and kidney disease risk were best described by daily minimum temperature or nighttime mean temperature, it might imply that the inability to recover from heat stress overnight plays a key role in conveying risk.

In epidemiologic studies of the relationship between temperature and kidney disease, dysnatremia and volume depletion (diagnostic disorders that may result from heat stress compromising the homeostatic capacity of the kidney to regulate salt and water balance, respectively (Feehally and Khosravi, 2015)) typically have not been included in analyses of kidney disease outcomes. Not taking these outcomes into account might lead to underestimation of the full impacts of temperature exposure on kidney health. Furthermore, dysnatremia or volume depletion (as potential manifestations of kidney disease) may constitute an initial diagnosis, followed later by diagnosis of a specific kidney disease (e.g., AKF). Inclusion of dysnatremia and volume depletion as secondary outcomes in studies of kidney disease subtypes could help more accurately estimate the true date of disease onset by using the date of the initial visit for dysnatremia or volume depletion instead of the date of the following visit for kidney disease, and therefore reduce exposure misclassification in the temporal dimension.

In this study, we hypothesized that there is an association between short-term temperature exposure and risk of kidney-related conditions, including AKF, urolithiasis, glomerular diseases (GD), renal tubulointerstitial diseases (TIN), CKD, dysnatremia, and volume depletion. We also evaluated the influence of the specification of the temperature variable in four dimensions: spatial resolution, absolute versus relative scale, incorporation of other meteorological variables, and intraday measures.

2. Material and methods

2.1. Outcome assessment

We obtained from the New York State (NYS) Department of Health Statewide Planning and Research Cooperative System encounter-level data on hospital visits (for patients $\geq$ 18 years of age), including emergency department (ED) visits and inpatient admissions, from 2007 to 2016. NYS covers 10 climate divisions (Fig. 1) based on the Climate Divisional Dataset from the National Oceanic and Atmospheric Administration (NOAA) (Vose et al., 2014). For each encounter, we obtained data on unique personal identifier, International Classification of Diseases, Ninth Revision, Clinical Modification (ICD-9-CM) (2007–2015) or Tenth Revision, Clinical Modification (ICD-10-CM) (2015–2016) principal diagnosis codes, date of admission and discharge, residential address, age, sex, race, ethnicity, and homelessness status indicator (i.e., homeless versus not known to be homeless).

In this study, we included seven kidney-related conditions based on the principal diagnosis code, including five kidney disease subtypes: AKF (ICD-10-CM: N17), urolithiasis (N20-N23), GD (N00-N08), TIN (N10-N16), and CKD (N18); and two kidney-related disorders: dysnatremia (E87.0 and E87.1) and volume depletion (E86). The ICD-9-CM counterpart codes are listed in **Table S1**. Cases with external causes of injury (e.g., transport accident, flood; coded with a different indicator than the principal diagnosis) were excluded from the main analysis, except cases with the external causes of natural heat/sunlight (ICD-9-CM: E9000, ICD-10-CM: X30XXXA and X32XXXA) and natural cold (ICD-9-CM: E9010, ICD-10-CM: X31XXXA); this exclusion was tested in a sensitivity analysis.

To best capture the date of a kidney condition event, and consequently the short-term temperature exposure time window that might have precipitated that event, we restricted our outcomes to unplanned encounters, including ED visits and emergency or urgent inpatient admissions. Planned, elective encounters might take place several days or more after the onset of the condition, resulting in an incorrect event onset date and exposure misclassification. We used the unique personal identifier to track each patient's history of unplanned encounters for

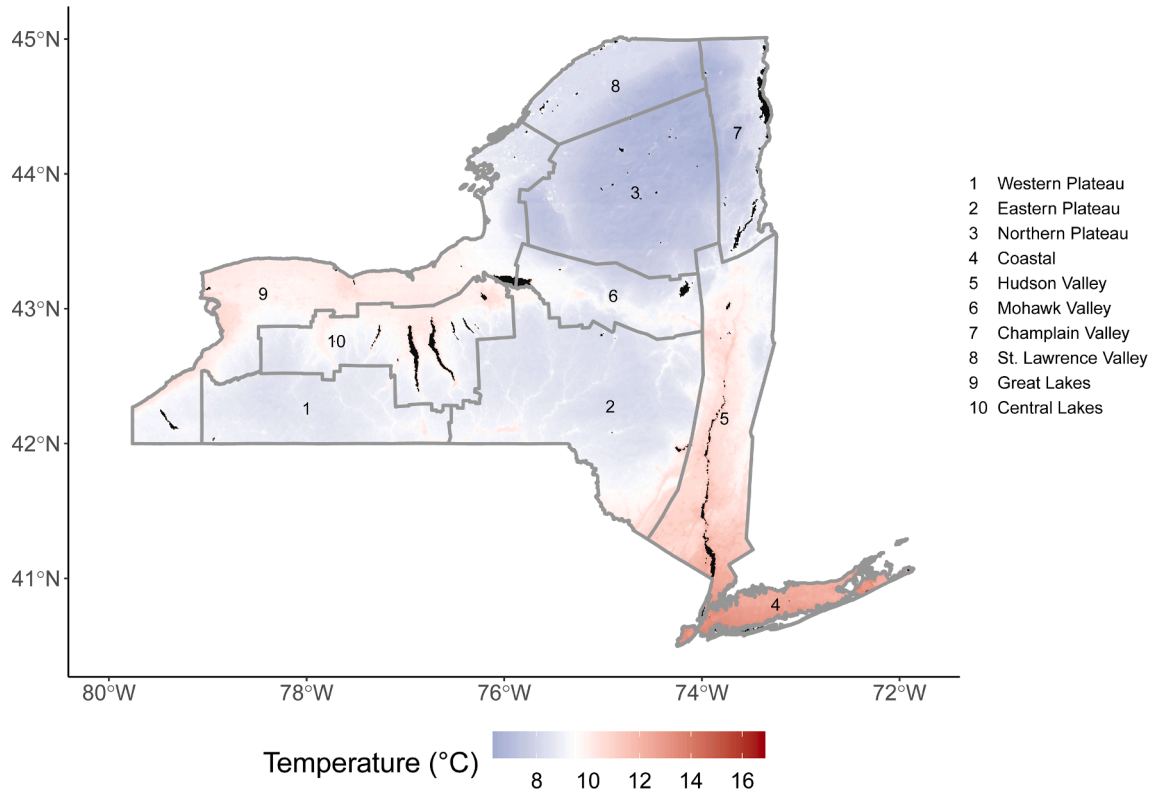

Fig. 1. Map of climate divisions (based on the Climate Divisional Dataset from the National Oceanic and Atmospheric Administration) and average dry-bulb temperature at 1 km × 1 km resolution using random forest models in New York State (2007–2016) (black color indicating missing values in water bodies).

kidney-related conditions and considered any series of such encounters with ≤ 30 days between the discharge date for an earlier encounter and the admission date for the next encounter to constitute a single occurrence. Although we did not include a few kidney disease codes (ICD-10-CM: N19, N25-N29; the corresponding ICD-9-CM codes are listed in **Table S1**.) in our primary outcomes, we did include them when determining whether a series of encounters constituted the same occurrence. We used the admission date and diagnosis code of the first encounter of each occurrence as the case date and diagnosis code for that occurrence. For example, if a patient had an unplanned visit for AKF on Day 0 (discharged on Day 5), another unplanned visit for ICD-10-CM N19 on Day 32, and a third unplanned visit for GD on Day 45, then these three visits would be considered a single occurrence with a case date of Day 0 and a diagnosis code of AKF.

Cases were geocoded with the NYS GIS Program Office Geocoding Service in ArcMap (version 10.8.1) and linked with exposure data.

2.2. Exposure assessment

We derived daily mean dry-bulb temperature at 1 km × 1 km resolution using random forest models (Jin et al., 2021). In these models, the dependent variable was monitored air temperature, obtained from NOAA (Chamberlain, 2020), and the independent predictors were satellite-based land surface temperature (Wan et al., 2015), elevation (NASA/METI/AIST/Japan Spacesystems and U.S./Japan ASTER Science Team, 2019), normalized difference vegetation index (Didan, 2015), land use type (Friedl and Sulla-Menashe, 2019); day of year, latitude, and longitude. More details on this modeling are presented in **Text S1 and Tables S2-3**. We then resampled the 1-km temperature data to obtain coarser exposure resolutions (5 km, 10 km, 20 km, and 35 km). We also derived daily mean dry-bulb temperature, dew point temperature, wind speed, and solar radiation at 0.1° × 0.1° resolution (approximately 8.2 km × 11.1 km) from ERA5-Land hourly data (Munoz Sabater, 1981). We calculated hourly relative humidity from the dew point temperature data (WMO, 2018), and obtained hourly specific humidity data at 0.125° × 0.125° resolution from the North American Land Data Assimilation System (NLDAS) (Xia et al., 2009; Xia et al., 2012).

We calculated the following temperature metrics incorporating other meteorological variables: wet-bulb temperature, heat index, humidex, net effective temperature, indoor WBGT, and outdoor WBGT. We first obtained hourly values for each metric using hourly data from ERA5-Land hourly data (Munoz Sabater, 1981). Among these metrics, outdoor WBGT incorporates dry-bulb temperature, humidity, wind speed, and solar radiation; net effective temperature incorporates dry-bulb temperature, humidity, and wind speed; and the other metrics incorporate dry-bulb temperature and humidity. More details on metric calculation methods are presented in **Text S2**. We then calculated daily mean, daily minimum, daily maximum, daytime mean, and nighttime mean values for each temperature metric. The daytime period was defined as 8 a.m. to 8 p.m. (Eastern Standard Time) and the nighttime period as 8 p.m. (the previous day) to 8 a.m.

2.3. Study design

We performed all statistical analyses with R (version 4.0.2). We received ethical clearances for this study from the Yale University Institutional Review Board (ID: 2000027748).

To assess associations between temperature exposure and kidney-related conditions, we used an individual-level symmetric bi-directional case-crossover design. For each hospital occurrence as defined above, we chose four control days exactly one and two weeks before and after the case date, such that patients served as their own controls. With such selection of controls, time-invariant individual characteristics (e.g., age, sex, and personal behaviors), day of week, and seasonal and long-term patterns were controlled for automatically.

We used conditional logistic regression with distributed lag non-linear models (DLNMs) to calculate odds ratios (OR) and 95%

confidence intervals (CI) for associations between temperature exposure and risk of kidney-related condition outcomes (Gasparrini, 2019). We restricted the maximum lag to lag 6 days to avoid overlapped exposure periods between cases and controls, and calculated cumulative odds ratios for lag 0–6 days. In all models, we adjusted for daily mean dew point temperature, wind speed, and solar radiation on the absolute scale. For temperature, we fitted a natural cubic spline with knots placed at 10^{th}, 75^{th} and 90^{th} percentiles (Gasparrini et al., 2015); for dew point temperature, wind speed, and solar radiation, we fitted a natural cubic spline with knots placed at 25^{th}, 50^{th} and 75^{th} percentiles. For the lag dimensions of cross-bases, we fitted natural cubic splines with knots equally placed at the log scale with degrees of freedom (df) = 3.

We selected condition-specific minimum morbidity temperature (MMT) values between the 1^{st} and the 99^{th} percentiles. In addition to showing OR estimates across the entire temperature range using exposure–response curves, we also reported OR estimates at the 1^{st}, 5^{th}, 20^{th}, 80^{th}, 95^{th}, and 99^{th} percentiles of temperature, respectively. When evaluating the influence of temperature specification in each of the four dimensions on exposure–response relationships and conducting effect modification or sensitivity analyses, we estimated ORs with the median temperature for the entire study period (2007–2016) as the reference temperature. We used the median temperature instead of the MMT for simplicity and ease of comparison, as MMT values could differ by temperature specification (i.e., spatial resolution, temperature scale, temperature metric, or intraday measure), across sub-groups of potential effect modifiers, and between the main analysis and each of the alternative sensitivity analyses. However, ultimately, for our main model, we used MMT as the reference temperature. MMT is the preferred reference temperature for showing association magnitudes (Gasparrini et al., 2015; Gasparrini et al., 2010).

Through a process described below in Methods and Results, we ultimately chose for our main model a one-stage model with daytime mean outdoor WBGT on the absolute scale as the temperature exposure.

2.4. Influence of temperature spatial resolution

We used daily mean dry-bulb temperature to assess the influence of temperature spatial resolution. We performed this assessment using the absolute temperature scale. We fitted models using temperature exposures at 1-, 5-, 10-, 20- and 35-km spatial resolution, and compared exposure–response patterns across these models, as well as model performance based on Akaike's information criterion (AIC) values (Burnham and Anderson, 2002). We considered a difference in AIC values between models of ≥ 10 to be meaningful, with lower AIC values indicating better model fit (Burnham and Anderson, 2002). As described in Results, we selected 10 km as the spatial resolution for assessment of absolute versus relative temperature scale.

To evaluate the role of spatial variability in daily mean dry-bulb temperature in the selection of spatial resolution, we estimated spatial variability using gridded temperature values at 1-km resolution. For each pair of 1-km grids, we calculated 1) the Pearson correlation coefficient between the two grid-specific time-series of daily mean temperature (2007–2016), and 2) the divergence between the two temperature time-series: $Divergence_{ij} = \sqrt{\sum_{d \in D_{ij}} \left(temp_{i,d} - temp_{j,d} \right)^2 / n_{ij}}$ (where D_{ij} is the set of days having temperature data for both grids i and j, $temp_{i,d}$ is the daily mean dry-bulb temperature value in grid i on day d, and n_{ij} is the number of days in D_{ij}) (Bell et al., 2011).

2.5. Influence of absolute versus relative temperature scale

To calculate the relative scale, we standardized temperature on the Celsius scale (i.e., absolute scale) into temperature quantiles (i.e., relative scale) based on climate-division-specific daily mean dry-bulb temperature distributions during the study period (2007–2016) (Guo et al., 2014). To assess the influence of temperature scale, we compared one-stage or two-stage (i.e., fitting division-specific DLNMs in the first stage and then pooled the cumulative exposure–response curves at lag 0–6 days by random-effects multivariate meta-analysis in the second stage (Gasparrini et al., 2012; Gasparrini and Armstrong, 2013)) models using temperature on the absolute or relative scale. When using temperature on the absolute scale either in one-stage or two-stage models, we placed the knots of temperature splines at fixed temperature values (i.e., −3.1 °C, 17.6 °C, and 20.8 °C for daily mean dry-bulb temperature in this analysis evaluating temperature scale; and −4.7 °C, 19.5 °C, and 23.2 °C for daytime mean outdoor WBGT in the main analysis) based on state-level temperature percentile values. When using temperature on the relative scale either in one-stage or two-stage models, we placed the knots of temperature splines at fixed quantile positions (i.e., 0.10, 0.75, and 0.90). We evaluated the heterogeneity across divisions by I^2 and the Q-statistics in the second stage of two-stage models. As described in Results, based on association patterns and heterogeneity statistics, we selected one-stage models using temperature on the absolute scale for our main model.

2.6. Influence of temperature metric and intraday measure

We first compared different temperature metrics incorporating other meteorological variables (i.e., daily mean dry-bulb temperature, wet-bulb temperature, heat index, humidex, net effective temperature, indoor WBGT, and outdoor WBGT) in separate models. As described in Results, based on model performance (i.e., AIC values), we selected outdoor WBGT for our main model. We then compared daily mean, daily minimum, daily maximum, daytime mean, and nighttime mean outdoor WBGT in separate models, and, again based on model performance, we selected daytime mean WBGT for our main model, as described in Results. We double checked the selection of outdoor WBGT by comparing daytime mean across dry-bulb temperature and the temperature metrics incorporating other meteorological variables. Furthermore, after selecting daytime mean outdoor WBGT, we re-assessed the influence of absolute versus relative outdoor WBGT scale.

2.7. Effect modification

We conducted stratified analyses to evaluate effect modification by calendar period (2007–2011 and 2012–2016), age (18–44, 45–64, and $\geq$ 65 years), sex (female and male), race (Asian, Black or African American, White, multi-racial, and other races and missing), ethnicity (Hispanic or Latino, not Hispanic or Latino, and unknown), homelessness status (homeless and not known to be homeless), and first- versus re-occurrence status. We assessed heterogeneity across sub-groups in multivariate random-effects meta-analyses by calculating I^2 and Q-statistics using the chi-squared test.

2.8. Sensitivity analyses

To assess the robustness of the results to the specifications of meteorological covariates (i.e., humidity, wind speed, and solar radiation), we performed sensitivity analyses on: (1) exclusion of the covariates (one at a time); (2) measurement of the covariates on absolute versus relative scale; (3) using different humidity metrics (i.e., dew point temperature, relative humidity, and specific humidity); and (4) using different intraday measures (e.g., daily maximum, nighttime mean) of the meteorological covariates.

Additionally, we performed the following sensitivity analyses: 1) using a time-stratified case-crossover design (i.e., control dates in the same month and on the same day of the week as case date) instead of the symmetric bi-directional design (although the potential for bias exists for both designs – overlap bias for the symmetric bi-directional design and bias from the step function assumption for the time-stratified design – it is difficult to determine the direction and magnitude of bias for

either design (Lu and Zeger, 2007), making a sensitivity analysis prudent); 2) using a lag period of lag 0–13 days instead of lag 0–6 days; 3) placing the knots in the temperature dimension at different sets of quantiles (25^{th}, 50^{th} and 75^{th}; 25^{th}, 65^{th}, and 90^{th}; 20^{th}, 40^{th}, 60^{th}, and 80^{th}; and 10^{th}, 25^{th}, 75^{th}, and 90^{th}); 4) varying the df in the lag dimension of the temperature cross-basis from 3 to 6; 5) placing the knots in the humidity, wind speed, or solar radiation dimension at different sets of quantiles (10^{th}, 75^{th}, and 90^{th}; 20^{th}, 40^{th}, 60^{th}, and 80^{th}; and 10^{th}, 25^{th}, 75^{th}, and 90^{th}); 6) including cases with external causes; and 7) excluding cases with low geocoding quality or low exposure assignment quality. In this study, we considered the addresses that could not be geocoded with the locator incorporating both the street number and the zip code (recommended by the NYS GIS Program Office) to have low geocoding quality and the addresses that were covered by a grid with missing exposure values to have low exposure assignment quality.

3. Results

3.1. Study characteristics

In this study, we included 1,209,934 ED visits and emergency or urgent inpatient admissions for kidney-related conditions, of which over 40% were urolithiasis (n = 519,297) and only about 0.3% were GD (n = 4,023) (Table 1). More than 80% of each kidney-related condition occurred in the Coastal, Hudson Valley, or Great Lakes climate division. The majority of cases of AKF (70.1%), dysnatremia (68.6%), and volume depletion (51.0%) were ≥ 65 years of age, whereas age 18–44 years was the modal age for urolithiasis (46.7%), GD (45.7%), and TIN (60.2%). Urolithiasis (59.2%) and CKD (57.2%) were more common in males than in females, whereas TIN (83.2%), dysnatremia (65.4%), and volume depletion (59.7%) were more common in females. Between 40.4% and 69.6% of cases of each condition occurred among Whites, with more than one-third (34.7%) of CKD cases occurring in the Black or African American race group. Between 71.2% and 84.9% of cases of each condition occurred in the non-Hispanic or Latino ethnicity group. Very few cases of each condition were homeless (ranging from 0.5% to 5.8%). For each condition, approximately 80% or more cases were first occurrences in our dataset, with the exception of CKD, for which only 60.7% were first occurrences. Of all occurrences, 92.9% (n = 1,123,773) only had a single hospital encounter.

The climate divisions in which most cases occurred were also the warmest divisions in NYS during 2007–2016. The Coastal division was the warmest (Fig. 1), with a median daily mean temperature of 12.8 °C (25^{th} – 75^{th} percentile: 4.9, 19.9 °C), followed by the Hudson Valley division (median = 10.6 °C; 25^{th} – 75^{th} percentile: 2.3, 18.6 °C) and the Great Lakes division (median = 9.7 °C; 25^{th} – 75^{th} percentile: 1.7, 18.2 °C) (Table S4). The coldest division was the Northern Plateau division (median = 8.1 °C; 25^{th} – 75^{th} percentile: −0.9, 16.3 °C).

Table 1
Hospital visits for kidney-related conditions (n = 1,209,934) in New York State (2007–2016).

	AKF	Urolithiasis	GD	TIN	CKD	Dysnatremia	Volume depletion
Total (n)	206,618	519,297	4,023	176,359	18,748	67,568	217,321
Climate division [n (%)]							
Western Plateau	4,096 (2.0)	11,693 (2.3)	51 (1.3)	2,967 (1.7)	270 (1.4)	1,632 (2.4)	6,358 (2.9)
Eastern Plateau	7,738 (3.7)	23,211 (4.5)	145 (3.6)	7,859 (4.5)	692 (3.7)	2,972 (4.4)	9,869 (4.5)
Northern Plateau	807 (0.4)	2,638 (0.5)	<11 (<0.3)[a]	696 (0.4)	59 (0.3)	319 (0.5)	1,192 (0.5)
Coastal	83,503 (40.4)	206,633 (39.8)	>1,855 (>46.1)[a]	69,788 (39.6)	7,383 (39.4)	26,550 (39.3)	77,386 (35.6)
Hudson Valley	66,253 (32.1)	145,576 (28.0)	1,323 (32.9)	55,554 (31.5)	6,317 (33.7)	19,423 (28.7)	64,786 (29.8)
Mohawk Valley	4,844 (2.3)	14,484 (2.8)	80 (2.0)	3,731 (2.1)	373 (2.0)	2,116 (3.1)	7,664 (3.5)
Champlain Valley	1,322 (0.6)	4,421 (0.9)	20 (0.5)	1,358 (0.8)	123 (0.7)	438 (0.6)	2,184 (1.0)
St. Lawrence Valley	1,475 (0.7)	6,348 (1.2)	22 (0.5)	2,100 (1.2)	260 (1.4)	628 (0.9)	2,116 (1.0)
Great Lakes	28,292 (13.7)	77,594 (14.9)	363 (9.0)	23,252 (13.2)	2,481 (13.2)	9,975 (14.8)	32,338 (14.9)
Central Lakes	8,288 (4.0)	26,699 (5.1)	153 (3.8)	9,054 (5.1)	790 (4.2)	3,515 (5.2)	13,428 (6.2)
Calendar period [n (%)]							
2007–2011	97,471 (47.2)	253,793 (48.9)	1,850 (46.0)	75,528 (42.8)	9,104 (48.6)	31,331 (46.4)	113,225 (52.1)
2012–2016	109,147 (52.8)	265,504 (51.1)	2,173 (54.0)	100,831 (57.2)	9,644 (51.4)	36,237 (53.6)	104,096 (47.9)
Age (years) [n (%)]							
18–44	12,729 (6.2)	242,702 (46.7)	1,837 (45.7)	106,112 (60.2)	3,269 (17.4)	3,979 (5.9)	55,644 (25.6)
45–64	49,033 (23.7)	210,994 (40.6)	1,199 (29.8)	45,281 (25.7)	7,474 (39.9)	17,251 (25.5)	50,776 (23.4)
≥65	144,855 (70.1)	65,598 (12.6)	985 (24.5)	24,953 (14.1)	8,004 (42.7)	46,336 (68.6)	110,892 (51.0)
Missing values	1 (0.0)	3 (0.0)	2 (0.0)	13 (0.0)	1 (0.0)	2 (0.0)	9 (0.0)
Sex [n (%)]							
Female	100,101 (48.4)	211,665 (40.8)	1,824 (45.3)	146,671 (83.2)	8,032 (42.8)	44,162 (65.4)	129,832 (59.7)
Male	106,516 (51.6)	307,629 (59.2)	2,199 (54.7)	29,686 (16.8)	10,715 (57.2)	23,405 (34.6)	87,489 (40.3)
Missing values	1 (0.0)	3 (0.0)	–	2 (0.0)	1 (0.0)	1 (0.0)	–
Race [n (%)]							
Asian	4,703 (2.3)	14,756 (2.8)	218 (5.4)	5,254 (3.0)	503 (2.7)	2,910 (4.3)	4,145 (1.9)
Black or African American	42,882 (20.8)	43,545 (8.4)	921 (22.9)	28,426 (16.1)	6,502 (34.7)	8,065 (11.9)	32,646 (15.0)
White	127,527 (61.7)	347,272 (66.9)	1,758 (43.7)	96,466 (54.7)	7,576 (40.4)	45,895 (67.9)	151,287 (69.6)
Multi-racial	8,067 (3.9)	25,752 (5.0)	270 (6.7)	7,294 (4.1)	1,462 (7.8)	2,491 (3.7)	4,814 (2.2)
Other races and missing	23,439 (11.3)	87,972 (16.9)	856 (21.3)	38,919 (22.1)	2,705 (14.4)	8,207 (12.1)	24,429 (11.2)
Ethnicity [n (%)]							
Hispanic or Latino	17,313 (8.4)	71,802 (13.8)	589 (14.6)	33,816 (19.2)	1,931 (10.3)	5,389 (8.0)	19,244 (8.9)
Not Hispanic or Latino	175,370 (84.9)	393,082 (75.7)	3,066 (76.2)	125,561 (71.2)	14,660 (78.2)	57,174 (84.6)	183,229 (84.3)
Unknown	13,935 (6.7)	54,413 (10.5)	368 (9.1)	16,982 (9.6)	2,157 (11.5)	5,005 (7.4)	14,848 (6.8)
Residence status [n (%)]							
Not known to be homeless	200,832 (97.2)	516,914 (99.5)	3,789 (94.2)	173,653 (98.5)	18,487 (98.6)	65,337 (96.7)	213,999 (98.5)
Homeless	5,786 (2.8)	2,383 (0.5)	234 (5.8)	2,706 (1.5)	261 (1.4)	2,231 (3.3)	3,322 (1.5)
Occurrence [n (%)]							
First occurrence	163,584 (79.2)	404,794 (78.0)	3,223 (80.1)	146,188 (82.9)	11,381 (60.7)	54,498 (80.7)	189,663 (87.3)
Re-occurrence	43,034 (20.8)	114,503 (22.0)	800 (19.9)	30,171 (17.1)	7,367 (39.3)	13,070 (19.3)	27,658 (12.7)

Note: Including emergency department visits, emergency inpatient admissions and urgent inpatient admissions. Hospital visits within 30 days (including 30 days) from the last unplanned visits are considered as the same occurrence and are not counted in this table. AKF, acute kidney failure; GD, glomerular diseases; TIN, renal tubulo-interstitial diseases; CKD, chronic kidney disease.

[a] Due to the small cell policy for confidentiality, the cell values in divisions Northern Plateau and Coastal were coarsened for GD.

3.2. Influence of temperature spatial resolution

Based on the cumulative exposure–response associations (Fig. S1), for each outcome, the difference across models using different spatial resolutions was negligible, compared with the uncertainty in the association estimates. Considering the irregular shapes and small areas of some climate divisions, the resolution of ERA5 data (i.e., 0.1° × 0.1° [approximately 8.2 km × 11.1 km]), and the meaningfully inferior model performance (based on AIC values) of 35 km resolution for AKF and of 1 km and 5 km resolutions for volume depletion (Table S5 and Text S3), we selected 10 km as the temperature exposure resolution in the following analysis for absolute versus relative temperature scale.

We observed high correlations of daily mean dry-bulb temperature between pairs of 1-km grids within 100 km of each other or less, and small median divergence in daily mean temperature between pairs of 1-km grids within 35 km of each other or less (Table S6), which may explain the similar exposure–response patterns across temperature resolutions (Fig. S1).

3.3. Influence of absolute versus relative temperature scale

When using daily mean dry-bulb temperature at 10 km resolution on the absolute scale, one-stage and two-stage models showed very similar exposure–response curves for each outcome (Fig. S2**A**), suggesting negligible heterogeneity across climate divisions. On the relative scale (i.e., division-specific temperature quantiles), one-stage and two-stage models also showed similar patterns, with the exception of AKF and TIN below the median temperature (Fig. S2**B**), suggesting a small degree of heterogeneity across divisions.

Furthermore, in the two-stage models on both the absolute and relative scales, we found no statistical heterogeneity across divisions (Table S7), confirming that one-stage models were sufficient. Given the slight heterogeneity between one-stage and two-stage models in exposure–response curves for two outcomes using the relative scale and the homogeneity for all outcomes using the absolute scale, we chose one-stage models using temperature on the absolute scale for further analyses.

3.4. Influence of temperature metrics and intraday measures

Although we derived daily mean dry-bulb temperature at high spatial resolution (i.e., 1 km) from random forest models, we did not have access to hourly dry-bulb temperature (to calculate intraday measures) or other meteorological variables (i.e., humidity, wind speed, and solar radiation) at this high level of resolution. Rather, to calculate temperature metrics incorporating other meteorological variables and intraday temperature measures, we used hourly dry-bulb temperature, dew point temperature, wind speed, and solar radiation at 0.1° × 0.1° resolution from ERA5-Land hourly data, such that ambient temperature used in the following analyses had a resolution of 0.1° × 0.1° (approximately 8.2 km × 11.1 km).

Temperature distributions using different metrics incorporating other meteorological variables or different intraday measures in NYS during the study period are shown in Table S8. Given the different ranges of temperature metrics or intraday measures, for fair comparison, we presented the association curves and reported the association estimates at specific quantiles of each measurement (e.g., we reported ORs at the 95th percentiles of daily mean dry-bulb temperature and daytime mean net effective temperature, instead of reporting ORs at 20 °C). However, we still used temperature on the absolute scale in the models. Furthermore, although we observed high correlation across temperature metrics or intraday measures, with Pearson correlation coefficients all above 0.90 (Tables S9-S11), we found different modeling performance and association patterns across these metrics/intraday measures.

First, we assessed the influence of daily mean temperature metrics incorporating other meteorological variables on model performance. For each condition, we considered the model with the minimum AIC value, along with the models with AIC values exceeding the minimum AIC value by < 10, to have good performance. Wet-bulb temperature and indoor WBGT showed good model performance for four of the seven kidney-related conditions; dry-bulb temperature, heat index, and humidex for five conditions; and net effective temperature and outdoor WGBT for six conditions (Table 2). The exception for net effective temperature was volume depletion, for which the AIC value exceeded the minimum AIC value by 20.3, whereas the exception for outdoor WBGT was dysnatremia, for which the AIC value exceeded the minimum AIC by 11.1. Furthermore, for dysnatremia, the deviance in association magnitudes between outdoor WBGT and the metrics with good statistical performance was smaller than the modeling uncertainty, whereas for volume depletion, the deviance in association magnitudes between outdoor WBGT (the only metric with good performance) and net effective temperature was larger than the modeling uncertainty (Fig. S3). While recognizing that each metric showed good performance for at least four of the seven outcomes, for simplicity, we tentatively selected outdoor WBGT for further analyses for all conditions.

We then compared daily mean, daily minimum, daily maximum, daytime mean, and nighttime mean measures of outdoor WBGT with respect to model performance. Daily maximum temperature showed good model performance for three of the seven kidney-related conditions; daily minimum and nighttime mean for four conditions; daily mean for five conditions; and daytime mean for all seven conditions (Table 2). While recognizing that each intraday measure showed good performance for at least three of the seven outcomes, for simplicity, we provisionally selected daytime mean outdoor WBGT for further analyses and as our reference metric for examining differences in association patterns across intraday temperature measures (Fig. 2). In the latter analysis, we observed substantial heterogeneity across intraday measures, especially for AKF, urolithiasis, and volume depletion, for which curves for several intraday measures fell outside of the daytime mean 95% CI. In addition, for AKF, urolithiasis, dysnatremia, and volume depletion, daytime mean temperature generally exhibited the highest ORs compared to other intraday temperature measures.

To further validate the selection of daytime mean outdoor WBGT as our temperature metric, we compared the seven temperature metrics incorporating other meteorological variables using the daytime mean instead of the daily mean, which we used in our initial selection of outdoor WBGT. Wet-bulb temperature showed good model performance for three kidney-related conditions; humidex and indoor WBGT for four conditions; dry-bulb temperature and heat index for five conditions; net effective temperature for six conditions, and outdoor WGBT for all seven conditions (Table S12). Thus, for daytime mean, each metric showed good performance for at least three of the seven outcomes. Furthermore, while all temperature metrics exhibited good model performance for the three outcomes that showed no association with daytime mean outdoor WBGT (i.e., GD, TIN, and CKD) and all but one metric (wet-bulb temperature) exhibited good performance for urolithiasis, only four metrics exhibited good performance for dysnatremia, two (outdoor WBGT and net effective temperature) for AKF, and one (daytime mean outdoor WBGT) for volume depletion. For parsimony, because outdoor WBGT showed good performance for all outcomes, we decided to retain daytime mean outdoor WBGT for our main model.

We note that the number of temperature metrics that fell outside of the outdoor WBGT 95% CI ranged from none for GD, TIN, CKD and dysnatremia to one for urolithiasis, three for AKF, and four for volume depletion (Fig. S4). and that for AKF, urolithiasis, dysnatremia, and volume depletion, outdoor WBGT exhibited the highest ORs (Fig. S4), except for wet-bulb temperature, which showed the poorest model performance based on AIC values for each of these conditions (Table S12).

We re-assessed the influence of absolute versus relative temperature scale using daytime mean outdoor wet-bulb globe temperature instead of daily mean dry-bulb temperature, which we used in our initial

Table 2
AIC values for kidney-related condition outcomes, from one-stage models using different daily mean temperature metrics incorporating other meteorological variables (i.e., dry-bulb temperature, wet-bulb temperature, heat index, humidex, net effective temperature, indoor wet-bulb globe temperature [WBGT], and outdoor WBGT) on the absolute scale or intraday measures (i.e., daily mean, daily minimum, daily maximum, daytime mean, and nighttime mean) of outdoor WBGT.

		AKF (n = 206,618)	Urolithiasis (n = 519,297)	GD (n = 4,023)	TIN (n = 176,359)	CKD (n = 18,748)	Dysnatremia (n = 67,568)	Volume depletion (n = 217,321)
Daily mean temperature metric	Dry-bulb temperature	664376.0 (17.3)[a]	1671137.3 (3.8)	12993.1 (2.6)	567675.7 (2.2)	60269.1 (3.2)	217304.6 (4.3)	697738.5 (62.0)
	Wet-bulb temperature	664397.8 (39.1)	1671141.2 (7.8)	12994.9 (4.4)	567675.2 (1.8)	60274.4 (8.5)	217320.4 (20.1)	697795.7 (119.3)
	Heat index	664361.4 (2.7)	1671137.6 (4.2)	12994.4 (3.9)	567674.5 (1.0)	60271.3 (5.3)	217311.1 (10.7)	697700.2 (23.8)
	Humidex	664372.0 (13.3)	1671136.5 (3.1)	12994.8 (4.3)	567673.5 (0.0)*	60272.0 (6.1)	217309.8 (9.4)	697727.2 (50.8)
	Net effective temperature	664358.7 (0.0)*	1671133.4 (0.0)*	12990.5 (0.0)*	567674.2 (0.8)	60265.9 (0.0)*	217300.4 (0.0)*	697696.7 (20.3)
	Indoor WBGT	664378.2 (19.5)	1671139.1 (5.7)	12994.6 (4.1)	567674.9 (1.5)	60271.6 (5.6)	217312.0 (11.6)	697742.0 (65.6)
	Outdoor WBGT	664365.7 (7.0)	1671134.3 (0.9)	12994.8 (4.3)	567674.8 (1.3)	60274.1 (8.2)	217311.5 (11.1)	697676.4 (0.0)*
Intraday measure of outdoor WBGT	Daily mean	664365.7 (14.0)	1671134.3 (1.1)	12994.8 (6.5)	567674.8 (5.0)	60274.1 (6.2)	217311.5 (0.0)*	697676.4 (105.4)
	Daily minimum	664498.4 (146.7)	1671179.2 (46.0)	12988.3 (0.0)*	567673.0 (3.3)	60267.9 (0.0)*	217313.8 (2.4)	698048.7 (477.7)
	Daily maximum	664400.3 (48.6)	1671135.1 (1.9)	12999.5 (11.2)	567671.0 (1.3)	60269.8 (1.9)	217326.6 (15.2)	697694.8 (123.8)
	Daytime mean	664351.8 (0.0)*	1671133.1 (0.0)*	12998.1 (9.9)	567672.8 (3.1)	60273.6 (5.7)	217317.0 (5.5)	697571.0 (0.0)*
	Nighttime mean	664420.7 (69.0)	1671162.9 (29.8)	12996.1 (7.8)	567669.7 (0.0)*	60273.3 (5.3)	217314.8 (3.3)	697981.1 (410.0)

Note: All models adjusted for daily mean dew point temperature, wind speed, and solar radiation (all on the absolute scale). AKF, acute kidney failure; GD, glomerular diseases; TIN, renal tubulo-interstitial diseases; CKD, chronic kidney disease.

[*] Disease-specific minimum AIC values when comparing temperature metrics incorporating other meteorological variables or intraday measures, respectively.

[a] Values in parentheses indicate the deviation from the disease-specific minimum AIC values. We considered a difference in AIC values between models of ≥ 10 to be meaningful, with lower AIC values indicating better model fit.

Table 3
Cumulative odds ratios (ORs) at lag 0–6 days with 95% confidence intervals (with the disease-specific minimum morbidity temperature [MMT] as the reference temperature) from one-stage models using daytime mean outdoor wet-bulb globe temperature on the absolute scale, in relation to risk for kidney-related condition outcomes.

	AKF (n = 206,618)	Urolithiasis (n = 519,297)	GD (n = 4,023)	TIN (n = 176,359)	CKD (n = 18,748)	Dysnatremia (n = 67,568)	Volume depletion (n = 217,321)
MMT percentile							
	22nd (0.4 °C)	1st (-13.5 °C)	99th (26.8 °C)	1st (-13.5 °C)	1st (-13.5 °C)	54th (12.3 °C)	1st (-13.5 °C)
OR at specific percentiles							
1st (-13.5 °C)	1.06	1.00	2.01	1.00	1.00	1.09	1.00
	(0.89, 1.26)	(ref)	(0.20, 20.35)	(ref)	(ref)	(0.73, 1.63)	(ref)
5th (-8.0 °C)	1.02	1.05	1.78	1.14	1.14	1.10	1.05
	(0.94, 1.11)	(0.99, 1.12)	(0.23, 13.44)	(1.02, 1.27)	(0.83, 1.56)	(0.82, 1.47)	(0.96, 1.15)
20th (-0.3 °C)	1.00	1.07	1.68	1.25	1.24	1.06	1.09
	(0.99, 1.01)	(0.97, 1.19)	(0.29, 9.76)	(1.03, 1.52)	(0.70, 2.18)	(0.87, 1.30)	(0.94, 1.28)
50th (10.6 °C)	1.03	1.08	1.71	1.25	1.19	1.00	1.15
	(0.94, 1.13)	(0.94, 1.24)	(0.50, 5.80)	(0.98, 1.60)	(0.59, 2.43)	(0.97, 1.03)	(0.94, 1.41)
80th (20.8 °C)	1.14	1.25	1.33	1.26	1.11	1.07	1.39
	(0.94, 1.37)	(1.05, 1.48)	(0.76, 2.32)	(0.93, 1.71)	(0.45, 2.75)	(0.91, 1.25)	(1.07, 1.80)
95th (24.7 °C)	1.36	1.41	1.10	1.29	1.19	1.26	1.88
	(1.09, 1.69)	(1.16, 1.70)	(0.85, 1.42)	(0.92, 1.81)	(0.43, 3.24)	(1.01, 1.59)	(1.41, 2.51)
99th (26.8 °C)	1.69	1.53	1.00	1.31	1.33	1.52	2.63
	(1.33, 2.14)	(1.25, 1.87)	(ref)	(0.93, 1.87)	(0.46, 3.83)	(1.17, 1.98)	(1.95, 3.57)

Note: Knots in all the models were 10th, 75th and 90th percentiles. All models were adjusted for daily mean dew point temperature, wind speed, and solar radiation (all on the absolute scale). AKF, acute kidney failure; GD, glomerular diseases; TIN, renal tubulo-interstitial diseases; CKD, chronic kidney disease; ref: the reference temperature (i.e., the disease-specific MMT).

selection of one-stage models on the absolute scale, and found our selection of one-stage models using temperature on the absolute scale to be robust (Fig. S5 and Table S13).

Therefore, we selected the one-stage model with daytime mean outdoor WBGT (at 0.1° × 0.1° resolution) on the absolute scale as the main model.

3.5. Temperature associations with risk for kidney-related conditions

In the main models using daytime mean outdoor WBGT as the temperature metric, the exposure–response pattern differed by kidney-related condition (Fig. 2 [solid red line] and Fig. S6). We observed no associations at lag 0–6 days for GD, TIN, or CKD. For AKF, urolithiasis, dysnatremia, and volume depletion, we observed graded increases in risk with increasing daytime mean outdoor WBGT, starting around 20–25 °C. For all conditions, we observed no increase in risk associated

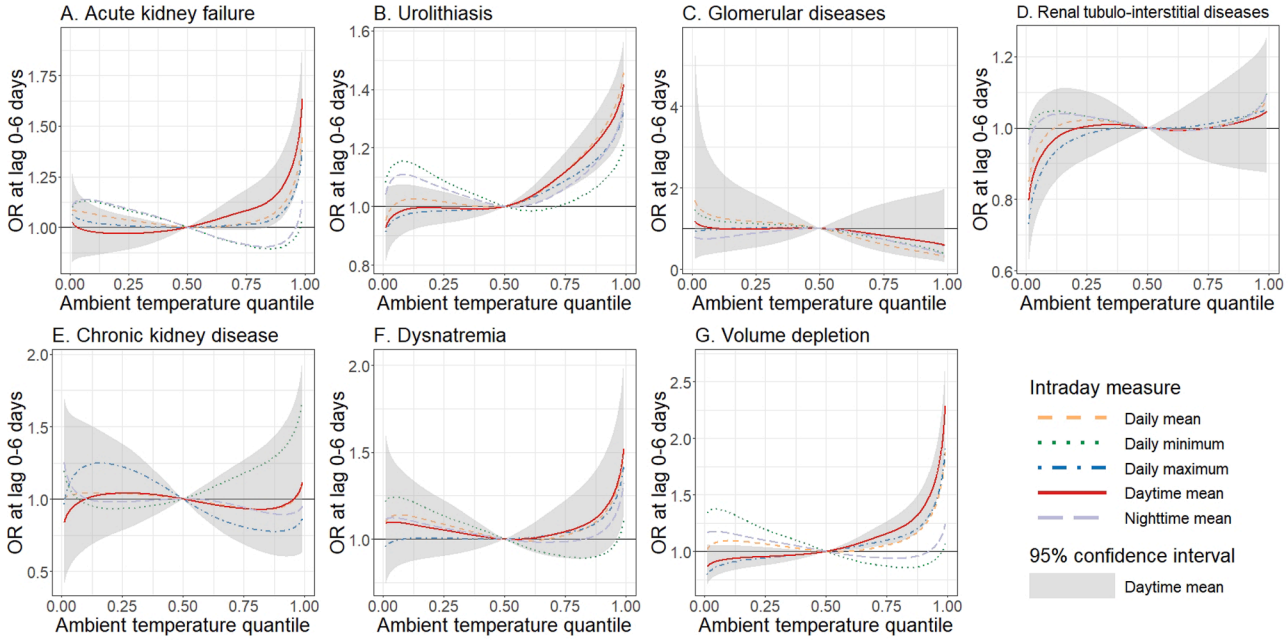

Fig. 2. Cumulative odds ratios (ORs) at lag 0–6 days with 95% confidence intervals (with the median of temperature distribution [2007–2016] as the reference temperature) from one-stage models using different intraday temperature measures (i.e., daily mean, daily minimum, daily maximum, daytime mean, and nighttime mean) of outdoor wet-bulb globe temperature (WBGT) on the absolute scale, in relation to risk for acute kidney failure (n = 206,618), urolithiasis (n = 519,297), glomerular diseases (n = 4,023), renal tubulo-interstitial diseases (n = 176,359), chronic kidney disease (n = 18,748), dysnatremia (n = 67,568), and volume depletion (n = 217,321). Temperature was fitted on the absolute scale in the models, but considering different ranges of different temperature measures, the temperature associations are shown on the relative scale. All models were adjusted for daily mean dew point temperature, wind speed, and solar radiation (all on the absolute scale).

with low temperatures.

With the condition-specific MMT value as the reference temperature, we observed ORs for heat exposure at the 95th percentile of daytime mean outdoor WBGT at lag 0–6 days to be 1.36 (95% confidence interval [CI]: 1.09, 1.69) for AKF, 1.41 (95% CI: 1.16, 1.70) for urolithiasis, 1.26 (95% CI: 1.01, 1.59) for dysnatremia, and 1.88 (95% CI: 1.41, 2.51) for volume depletion (Table 3). For more extreme heat exposure at the 99th percentile the ORs were elevated further: 1.69 (95% CI: 1.33, 2.14) for AKF, 1.53 (95% CI: 1.25, 1.87) for urolithiasis, 1.52 (95% CI: 1.17, 1.98) for dysnatremia, and 2.63 (95% CI: 1.95, 3.57) for volume depletion. For milder heat exposure at the 80th percentile, we observed elevated ORs for urolithiasis (OR = 1.25; 95% CI: 1.05, 1.48) and volume depletion (OR = 1.39; 95% CI: 1.07, 1.80).

3.6. Effect modification and sensitivity analyses

Taking into account the Bonferroni correction for multiple comparisons (corrected p-value = 0.05/[7 conditions × 7 potential effect modifiers]≈0.001), we did not observe significant heterogeneity by calendar period, age, sex, race, ethnicity, homelessness status, or first- versus re-occurrence status (**Figs. S7-S13**). Our findings were robust in all the sensitivity analyses (**Tables S14-S16 and Figs. S14-S23**).

4. Discussion

To assess the association between short-term temperature exposure (lag 0–6 days) and risk of seven kidney-related conditions in NYS, we first evaluated the influence of 1) measuring temperature at different spatial resolutions; 2) measuring temperature on the absolute versus relative scale; 3) using temperature metrics that incorporate other meteorological variables; and 4) using different intraday measures of temperature. This evaluation led us to model daytime mean outdoor WBGT measured at 0.1° × 0.1° resolution on the absolute scale for all seven outcomes. Furthermore, we chose to use one-stage models because we found minimal heterogeneity across climate divisions.

Our models revealed associations between higher short-term daytime mean outdoor WBGT exposure and increased risk for AKF, urolithiasis, dysnatremia, and volume depletion, with volume depletion exhibiting the strongest association. We did not observe associations for GD, TIN, or CKD.

4.1. Influence of spatial resolution and temperature scale

We observed similar association estimates across spatial resolutions ranging from 1 km to 35 km. In evaluating the association between short-term temperature exposure and all-cause mortality, Wu et al. and de Schrijver et al. observed that association estimates did not vary meaningfully across resolutions ranging from 1 km to zip-code-level and from below 5 km to approximately 28 km, respectively, consistent with our findings (Wu et al., 2019; de Schrijver et al., 2021).

The optimal spatial resolution for exposure assessment depends on both spatial variability in exposure and human mobility. We found little spatial variability in temperature over a range of 100 km, especially within the same climate division, which likely explains the lack of variability in association estimates across spatial resolutions. Previous studies reported that the median daily travel range (i.e., the shortest linear distance) in New York City and ten neighboring counties was 6.1 km in Spring (25th-75th percentile: 2.1, 13.0 km) and 4.2 km in Winter (25th-75th percentile: 1.1, 10.1 km) (Isaacman et al., 2010; Isaacman et al., 2011), which may support the slightly better performance of intermediate resolutions (i.e., 10 km and 20 km) in our study. Further research is needed on optimizing the spatial resolution of temperature exposure measurements in epidemiologic studies, taking into account both spatial variability in temperature exposure and human mobility.

Spatial variability in temperature was considerably greater across climate divisions than on a local scale (i.e., over a range of 100 km). However, for each outcome, when measuring temperature on an absolute scale, we observed negligible heterogeneity in association estimates across divisions, whether assessed by visually comparing exposure–response curves for one-stage versus two-stage models or by formal statistical tests. When temperature was measured on a relative scale, we observed a small degree of heterogeneity in exposure–response curves for two outcomes. Thus, we found the absolute scale to be marginally superior, with no advantage to using the relative scale, suggesting a lack of heterogeneity in adaptation across climate divisions in NYS. Further comparisons of absolute versus relative scale are warranted, especially in studies involving larger geographical areas or multiple locations.

4.2. Influence of temperature metrics

The number of daytime mean temperature metrics exhibiting good model performance ranged from only one (outdoor WBGT) for volume depletion to two for AKF to four for dysnatremia to six for urolithiasis, to all seven for GD, TIN, and CDK (**Table S12**). Thus, for the latter three kidney-related conditions (the three outcomes that showed no association with temperature exposure), model performance based on AIC provided no guidance about a preferred temperature metric to model, with all seven metrics being essentially equivalent. Regarding the four outcomes for which we observed elevated risk associated with high-temperature exposure, for urolithiasis, we could only rule out wet-bulb temperature based on AIC and for dysnatremia, we could rule out wet-bulb temperature, humidex, and indoor WBGT. However, for AKF, only two metrics (net effective temperature and outdoor WBGT) were acceptable based on AIC, and for volume depletion, only one metric (outdoor WBGT) was acceptable. Furthermore, for a given outcome, differences in model performance among temperature metrics can be associated with substantial differences in exposure–response curves among metrics (**Fig. S3**), underlining the importance of the choice of which metric to model in situations where there is meaningful heterogeneity in model performance across metrics.

Daytime mean outdoor WBGT, which incorporates humidity, wind, speed, and solar radiation, showed good model performance for all seven kidney-related conditions, and net effective temperature, which incorporates humidity and wind speed, showed good model performance for all but one condition (volume depletion). The superior model performance of these metrics suggests the importance of taking humidity, wind speed, and solar radiation into account in assessing kidney-related heat stress even after simply adjusting for these variables, which we did in our models.

Goldie et al. and Ross et al. found that combined temperature-humidity metrics (apparent temperature and simplified WBGT [incorporating humidity only] in Goldie et al. and wet-bulb temperature and heat index in Ross et al.) exhibited better model performance than dry-bulb temperature for renal disease hospital admissions in Australia and hospital visits for kidney stones in the U.S., respectively (Goldie et al., 2018; Ross et al., 2018). Adeyeye et al., Fletcher et al., and McTavish et al. found divergence in association estimates across temperature metrics for AKF morbidity in the U.S., the U.S., and Canada, respectively, with dry-bulb temperature (compared with heat index), dry-bulb temperature (compared with apparent temperature), and humidex (compared with dry-bulb temperature) exhibiting stronger associations, respectively (McTavish et al., 2018; Adeyeye et al., 2019; Fletcher et al., 2012). However, a Vietnamese study observed no differential model performance (based on AIC) between daily mean dry-bulb temperature and heat index for GD, TIN, CKD, and urolithiasis hospital admissions (Chu et al., 2022). Further research is warranted to assess whether, for each of the seven kidney-related conditions, our findings on model performance and association magnitudes using the various temperature metrics are reproducible/generalizable.

4.3. Influence of intraday temperature measures

For outdoor WBGT, the number of intraday measures exhibiting good model performance ranged from only one (daytime mean) for AKF and volume depletion to three for urolithiasis to four for GD and dysnatremia to all five for TIN and CDK. Thus, for the three outcomes not associated with temperature exposure (i.e., GD, TIN, and CKD), model performance based on AIC provided little or no guidance about a preferred intraday measure to model. Regarding the four outcomes for which we observed elevated risk associated with high-temperature exposure, for dysnatremia, we could only rule out daily maximum temperature based on AIC and for urolithiasis, we could rule out daily minimum and nighttime mean. For AKF and volume depletion, only daytime mean was acceptable based on AIC.

As with temperature metrics, it is important to point out that for a given outcome, differences in model performance among intraday measures can be associated with substantial differences in exposure–response curves among intraday measures (Fig. 2), underlining the importance of the choice of which intraday measure to model. That daytime mean temperature generally exhibited the strongest association with risk for AKF, urolithiasis, dysnatremia, and volume depletion suggests that accumulation of heat stress during the daytime (as opposed to recovery from heat stress overnight) is especially relevant in precipitating hospital visits for kidney-related conditions. Research using hourly temperature as the exposure could provide additional insights.

For AKF hospital admissions in the U.S., Fletcher et al. found daily mean dry-bulb temperature, compared with daily minimum and daily maximum, to exhibit the strongest association (Fletcher et al., 2012). Similarly, Ostro et al. found daily mean apparent temperature, compared with daily minimum and daily maximum, to exhibit the strongest association with hospitalization for AKF in the U.S. (Ostro et al., 2010). In a Chinese study, Yang et al. found that among daily mean, daily minimum, and daily maximum dry-bulb temperature, daily mean showed the strongest association with emergency ambulance dispatches for renal colic at the 90th percentile, and daily mean and daily minimum showed the strongest associations at the 99th percentile (Yang et al., 2015). However, for urolithiasis, AKF and CKD hospital admissions, Borg et al. found daily minimum dry-bulb temperature, compared with daily mean and daily maximum, to exhibit the strongest associations (Borg et al., 2017). Finally, for renal hospital admissions, an Australian study found that the model performance and the association magnitude rank using daily mean, minimum and maximum measures differed by geographic location (Goldie et al., 2018). Interestingly, we are unaware of previous studies that have examined daytime mean temperature in relation to risk for kidney-related conditions. These studies, in conjunction with ours, suggest that different intraday measures result in different association estimates. As with temperature metrics, further research is needed to assess whether for each of the seven kidney-related conditions, our findings on model performance and association magnitudes for the different intraday temperature measures are reproducible/generalizable.

4.4. High-Temperature associations with risk for kidney diseases

The epidemiologic literature contains more evidence on the relationship between exposure to high temperature and risk for AKF and urolithiasis than for GD, TIN, or CKD. Kim et al. observed relative risk (RR) estimates for AKF ED admission ranging from 1.08 to 1.23 at the 90th percentile and ORs ranging from 1.09 to 1.43 at the 99th percentile of daily mean dry-bulb temperature at lag 0–6 days compared with district-specific MMT values in 16 districts in South Korea (Kim et al., 2018). Reid et al. observed 5% to 23% higher risk across five states for AKF hospital admissions on extreme heat days (defined by daily maximum dry-bulb temperature $\geq$ 95th percentile) than on non-extreme heat days in a U.S. study (Reid et al., 2012). Vaneckova and Bambrick found no increased risk for AKF hospital admissions on "hot" days (defined by daily mean dry-bulb temperature $\geq$ 95th percentile), but 25% (95% CI: 2%, 54%) increased risk on "very hot" days (defined by $\geq$ 99th percentile) in an Australian study (Vaneckova and Bambrick, 2013). Isaksen et al. found an RR of 1.68 (95% CI: 1.41, 2.01) on heat days (defined by daily maximum humidex $>$ 99th percentile) for AKF hospital admissions in a U.S. study (Isaksen et al., 2015). Other studies found elevated morbidity risk for AKF during heatwave events, with effect sizes varying partially due to different heatwave definitions (Chen et al., 2017; McTavish et al., 2018; Bobb et al., 2014; Borg et al., 2019; Hansen et al., 2008; Hopp et al., 2018; Lindstrom et al., 2013; Mangoni et al., 2017; Sherbakov et al., 2018; Fuhrmann et al., 2016). A recent meta-analysis reported an RR for AKF morbidity risk of 1.012 (95% CI: 1.009, 1.015) per 1 °C increase in temperature (Liu et al., 2021).

For emergency ambulance dispatches for urolithiasis, in a Chinese study, Yang et al. estimated RRs at lag 0–7 days to be 1.92 and 2.45 at the 90th and the 99th percentiles of daily mean dry-bulb temperature, respectively, with MMT as the reference temperature (Yang et al., 2015). In a U.S. study on hospital presentations (aged 20–65 years) for kidney stone, Ross et al. found an RR of approximately 1.10 over lag 0–10 days at the 99th percentiles compared with the 50th percentile of daily mean temperature (dry-bulb, wet-bulb, or heat index) during the summer (Ross et al., 2018). In another U.S. study, Vicedo-Cabrera et al. observed cumulative RRs over 10 days for urolithiasis ED presentations to be 1.35 and 1.48 at the 90th and the 99th percentiles of daily maximum wet-bulb temperature, respectively, with the 20th percentile as the reference (Vicedo-Cabrera et al., 2020). Borg et al. and Wilson et al. in two Australian studies observed increased hospital admission risk for urolithiasis associated with heat wave days, while Bobb et al. in a U.S. study found no such association among the elderly (Borg et al., 2019; Wilson et al., 2013; Bobb et al., 2014). A recent meta-analysis found an RR for urolithiasis morbidity risk of 1.022 (95% CI: 1.016, 1.027) per 1 °C increase in temperature (Liu et al., 2021).

In summary, our study and previous epidemiologic evidence support associations between short-term exposure to high temperature and risk for both AKF and urolithiasis.

For CKD morbidity risk associated with high ambient temperature exposure, three previous U.S. studies found null associations among the entire population or the elderly, similar to our results (Bobb et al., 2014; Fletcher et al., 2012; Malig et al., 2019). However, an Australian study observed statistically significant (i.e., $p < 0.05$) incidence rate ratios per 1 °C increase in dry-bulb temperature ranging from 1.01 to 1.02 for some single lag days from lag 0 to lag 5 days (Borg et al., 2017). The incidence rate ratios varied by lag days, hospital visit type, and intraday temperature measure (i.e., daily mean, maximum, or minimum) (Borg et al., 2017). For emergency room visits for chronic renal failure, a Chinese study found a relative risk estimate of 2.36 (95% CI: 1.33, 4.19) at 32 °C of 4-day average temperature, with 18 °C (i.e., the minimum morbidity temperature) as the reference (Wang and Lin, 2014). Additionally, a Vietnamese study reported an OR for risk of CKD hospital admission of 1.12 (95% CI: 1.00, 1.24) per 1 °C increase in daily mean dry-bulb temperature at lag 0–6 days (Chu et al., 2022). In an Australian study, Borg et al. found divergent associations between exposure to heat wave events and risk for ED or inpatient admissions for CKD (ranging from null to RR = 1.66 [95% CI: 1.11, 2.47]), depending on the heat wave definition, admission type, and sub-population (i.e., age $<$ 65 years versus $\geq$ 65 years; females versus males) (Borg et al., 2019). Further research is needed to clarify the relationship between ambient temperature exposure and CKD risk.

Only one previous study evaluated the relationships between short-term exposure to high temperature and risk for GD and TIN, reporting ORs per 1 °C increase in daily mean dry-bulb temperature at lag 0–6 days of 1.07 (95% CI: 0.99, 1.16) for GD and 1.06 (95% CI: 0.96, 1.17) for TIN (Chu et al., 2022). These null results were consistent with the null results in the current study. However, given the paucity of studies, further research is warranted in different regions to add to existing evidence.

4.5. High-temperature associations with dysnatremia and volume depletion

Excessive sweating due to exposure to high ambient temperature may cause both water and salt loss, leading to volume depletion and/or dysnatremia (Lipman et al., 2021). Volume depletion and dysnatremia may result in kidney injury and also may be manifestations of kidney disease (Feehally and Khosravi, 2015; Lombardi et al., 2021; Lee et al., 2016; Adams et al., 2011; McCullough, 2010; Combs and Berl, 2014). Many previous studies have revealed an association between high temperature exposure and increased volume depletion (or dehydration) risk (Sherbakov et al., 2018; Basu and Green, 2012; Ye et al., 2012), which is consistent with our findings. However, epidemiologic evidence is far from sufficient on the magnitude of high-temperature associations with volume depletion or dysnatremia.

4.6. Strengths and limitations

This study had several strengths. First, using random forest models, we obtained daily 1 km × 1 km resolution temperature estimates, enabling us to compare spatial resolutions across a range from highly-resolved to coarser using the same temperature data source, ruling out the influence of potential systematic differences among data sources. Second, for a more complete estimation of the impact of temperature exposure on kidney health, in addition to examining kidney diseases, we examined the kidney-related disorders of dysnatremia and volume depletion. Third, based on unique personal identifiers, we consolidated neighboring visits for kidney-related conditions (including dysnatremia and volume depletion) into a single occurrence. This approach improved our estimation of the date of diagnosis for each occurrence, reducing exposure misclassification. It also reduced the risk of dilution of associations by including as cases encounters that were more likely to have been triggered by existing disease than by temperature exposure.

Our study also had limitations. First, we had no data on human mobility to support the selection of spatial resolution. Second, we used the diagnosis code of the first encounter of each occurrence as the diagnosis code for that occurrence; however, a later diagnosis code during that occurrence may have been the correct code. Third, climate variability in NYS is limited and further research covering geographic regions with greater climate variability is warranted. Fourth, we had no information on patient encounters prior to 2007, such that the first occurrence of a kidney-related condition during the study period for a given patient actually could have been a re-occurrence during the patient's lifetime, leading to misclassification of re-occurrences as first occurrences. Fifth, lower geocoding quality for homeless patients based on coarse address description may lead to temperature exposure misclassification, and exclusion of homeless patients with missing addresses may lead to selection bias. In addition, homeless patients may have been included in the not-known-to-be homeless category.

5. Conclusions

We evaluated the influence of the specification of the temperature variable in four dimensions on estimation of the association between short-term temperature exposure and risk for unplanned hospital encounters for seven kidney-related conditions. We found temperature metric and intraday temperature measure to have considerably greater influence on the estimation of temperature associations than spatial resolution and temperature scale, which had little influence. For parsimony, we chose to model daytime mean outdoor WBGT, which showed good model performance for all outcomes. However, we note that daytime mean net effect temperature had good model performance for all outcomes except volume depletion.

We found that high daytime mean outdoor WBGT exposure over one week was a risk factor for unplanned hospital encounters for acute kidney failure, urolithiasis, dysnatremia, and volume depletion, but not for glomerular diseases, renal tubulo-interstitial diseases, and chronic kidney disease. For the three conditions not associated with temperature exposure, almost all metrics and intraday measures showed good model performance. However, for the four conditions associated with temperature exposure, in general there was considerably greater variability in model performance by temperature metric or intraday measure, especially for acute kidney failure and volume depletion. The differential model performance across the various temperature metrics incorporating other meteorological variables and the various intraday measures points toward the importance of careful selection of exposure metrics when estimating temperature-related health burden and designing heat alert systems.

CRediT authorship contribution statement

Lingzhi Chu: Conceptualization, Methodology, Software, Validation, Data curation, Formal analysis, Writing – original draft, Visualization. **Kai Chen:** Methodology, Writing – review & editing. **Susan Crowley:** Methodology, Writing – review & editing. **Robert Dubrow:** Conceptualization, Methodology, Writing – review & editing, Supervision, Project administration.

Declaration of Competing Interest

The authors declare that they have no known competing financial interests or personal relationships that could have appeared to influence the work reported in this paper.

Data availability

The authors do not have permission to share data.

Acknowledgments

Lingzhi Chu received a scholarship from the Dan David Prize. Robert Dubrow received support from the High Tide Foundation.

The funders had no role in data collection, study design, statistical analysis, decision to publish, or preparation of the manuscript.

This publication was produced from raw data purchased from the New York State Department of Health (NYSDOH). However, the conclusions derived, and views expressed herein are those of the author(s) and do not reflect the conclusions or views of NYSDOH. NYSDOH, its employees, officers, and agents make no representation, warranty or guarantee as to the accuracy, completeness, currency, or suitability of the information provided here.

Appendix A. Supplementary data

Supplementary data to this article can be found online at https://doi.org/10.1016/j.envint.2023.107783.

References

Adams, D., de Jonge, R., van der Cammen, T., Zietse, R., Hoorn, E.J., 2011. Acute kidney injury in patients presenting with hyponatremia. J. Nephrol. 24 (6), 749.

Adeyeye, T.E., Insaf, T.Z., Al-Hamdan, M.Z., Nayak, S.G., Stuart, N., DiRienzo, S., et al., 2019. Estimating policy-relevant health effects of ambient heat exposures using spatially contiguous reanalysis data. Environ. Health 18 (1), 35.

Basu, R., Green, R., 2012. The effect of high ambient temperature on emergency room visits. Epidemiology 23 (6), 813–820.

Bell, M.L., Ebisu, K., Peng, R.D., 2011. Community-level spatial heterogeneity of chemical constituent levels of fine particulates and implications for epidemiological research. J. Eposure Sci. Environ. Epidemiol. 21 (4), 372–384.

Bobb, J.F., Obermeyer, Z., Wang, Y., Dominici, F., 2014. Cause-specific risk of hospital admission related to extreme heat in older adults. JAMA 312 (24), 2659–2667.

Borg, M., Bi, P., Nitschke, M., Williams, S., McDonald, S., 2017. The impact of daily temperature on renal disease incidence: an ecological study. Environ. Health 16 (1), 114.

Borg, M., Nitschke, M., Williams, S., McDonald, S., Nairn, J., Bi, P., 2019. Using the excess heat factor to indicate heatwave-related urinary disease: a case study in Adelaide, South Australia. Int. J. Biometeorol. 63 (4), 435–447.
Burnham, K., Anderson, D., 2002. Model Selection and Multimodel Inference: A Practical Information-Theoretic Approach (2nd Edition). Springer, New York, pp. 70–72.
Chamberlain S. rnoaa:"NOAA" Weather Data from R (R package version 1.2.0). 2020.
Chen, T., Sarnat, S.E., Grundstein, A.J., Winquist, A., Chang, H.H., 2017. Time-series analysis of heat waves and emergency department visits in Atlanta, 1993 to 2012. Environ. Health Perspect. 125 (5), 057009.
Chu, L., Phung, D., Crowley, S., Dubrow, R., 2022. Relationships between short-term ambient temperature exposure and kidney disease hospitalizations in the warm season in Vietnam: A case-crossover study. Environ. Res. 112776.
Combs, S., Berl, T., 2014. Dysnatremias in patients with kidney disease. Am. J. Kidney Dis. 63 (2), 294–303.
de Schrijver, E., Folly, C.L., Schneider, R., Royé, D., Franco, O.H., Gasparrini, A., et al., 2021. A comparative analysis of the temperature-mortality risks using different weather datasets across heterogeneous regions. GeoHealth. 5, 5, e2020GH000363.
Didan K., 2015. MODIS/Terra vegetation Indices Monthly L3 Global 1km SIN Grid V006. In: DAAC NELP, editor.
Feehally, J., Khosravi, M., 2015. Effects of acute and chronic hypohydration on kidney health and function. Nutr. Rev. 73 (suppl_2), 110–119.
Fletcher, B.A., Lin, S., Fitzgerald, E.F., Hwang, S.A., 2012. Association of summer temperatures with hospital admissions for renal diseases in New York State: a case-crossover study. Am. J. Epidemiol. 175 (9), 907.
Friedl, M., 2019. Sulla-Menashe D. MCD12Q1 MODIS/Terra+Aqua Land Cover Type Yearly L3 Global 500m SIN Grid V006. In: DAAC NELP, editor.
Fuhrmann, C.M., Sugg, M.M., Konrad, C.E., Waller, A., 2016. Impact of extreme heat events on emergency department visits in North Carolina (2007–2011). J. Community Health 41 (1), 146–156.
García-Arroyo, F.E., Cristóbal, M., Arellano-Buendía, A.S., Osorio, H., Tapia, E., Soto, V., et al., 2016. Rehydration with soft drink-like beverages exacerbates dehydration and worsens dehydration-associated renal injury. American Journal of Physiology-Regulatory, Integrative Comparative. Physiology.
García-Arroyo, F.E., Tapia, E., Blas-Marron, M.G., Gonzaga, G., Silverio, O., Cristóbal, M., et al., 2017. Vasopressin mediates the renal damage induced by limited fructose rehydration in recurrently dehydrated rats. Int. J. Biol. Sci. 13 (8), 961.
Gasparrini, A., Armstrong, B., 2013. Reducing and meta-analysing estimates from distributed lag non-linear models. BMC Med. Res. Method. 13 (1), 1–10.
Gasparrini, A., Armstrong, B., Kenward, M.G., 2010. Distributed lag non-linear models. Stat. Med. 29 (21), 2224–2234.
Gasparrini, A., Armstrong, B., Kenward, M.G., 2012. Multivariate meta-analysis for non-linear and other multi-parameter associations. Stat. Med. 31 (29), 3821–3839.
Gasparrini, A., Guo, Y., Hashizume, M., Lavigne, E., Zanobetti, A., Schwartz, J., et al., 2015. Mortality risk attributable to high and low ambient temperature: a multicountry observational study. Lancet 386 (9991), 369–375.
Gasparrini A. Extensions of the dlnm package. 2019.
Goldie, J., Alexander, L., Lewis, S.C., Sherwood, S.C., Bambrick, H., 2018. Changes in relative fit of human heat stress indices to cardiovascular, respiratory, and renal hospitalizations across five Australian urban populations. Int. J. Biometeorol. 62 (3), 423–432.
Guo, Y., Gasparrini, A., Armstrong, B., Li, S., Tawatsupa, B., Tobias, A., et al., 2014. Global variation in the effects of ambient temperature on mortality: a systematic evaluation. Epidemiology 25 (6), 781.
Hansen, A.L., Bi, P., Ryan, P., Nitschke, M., Pisaniello, D., Tucker, G., 2008. The effect of heat waves on hospital admissions for renal disease in a temperate city of Australia. Int. J. Epidemiol. 37 (6), 1359–1365.
Heidari, L., Winquist, A., Klein, M., O'Lenick, C., Grundstein, A., Ebelt Sarnat, S., 2016. Susceptibility to heat-related fluid and electrolyte imbalance emergency department visits in Atlanta, Georgia, USA. Int. J. Environ. Res. Publ. Health. 13, 10.
Holt, S., Moore, K., 2001. Pathogenesis and treatment of renal dysfunction in rhabdomyolysis. Intensive Care Med. 27 (5), 803–811.
Hopp, S., Dominici, F., Bobb, J.F., 2018. Medical diagnoses of heat wave-related hospital admissions in older adults. Prev. Med. 110, 81–85.
Isaacman, S., Becker, R., Cáceres, R., Kobourov, S., Rowland, J., Varshavsky, A. (Eds.). A tale of two cities. Proceedings of the eleventh workshop on mobile computing systems & applications.
Isaacman, S., Becker, R., Cáceres, R., Kobourov, S., Martonosi, M., Rowland, J., et al. (Eds.). Ranges of human mobility in Los Angeles and New York. 2011 IEEE international conference on pervasive computing and communications workshops (PERCOM workshops), IEEE.
Isaksen, T.B., Yost, M.G., Hom, E.K., Ren, Y., Lyons, H., Fenske, R.A., 2015. Increased hospital admissions associated with extreme-heat exposure in King County, Washington, 1990–2010. Rev. Environ. Health 30 (1), 51–64.
Jimenez, C.A.R., Ishimoto, T., Lanaspa, M.A., Rivard, C.J., Nakagawa, T., Ejaz, A.A., et al., 2014. Fructokinase activity mediates dehydration-induced renal injury. Kidney Int. 86 (2), 294–302.
Jin, Z., Ma, Y., Chu, L., Liu, Y., Dubrow, R., Chen, K., 2021. Predicting spatiotemporally-resolved mean air temperature over Sweden from satellite data using an ensemble model. Environ. Res. 111960.
Kim, E., Kim, H., Kim, Y.C., Lee, J.P., 2018. Association between extreme temperature and kidney disease in South Korea, 2003–2013: Stratified by sex and age groups. Sci. Total Environ. 642, 800–808.
Kloog, I., Nordio, F., Coull, B.A., Schwartz, J., 2014. Predicting spatiotemporal mean air temperature using MODIS satellite surface temperature measurements across the Northeastern USA. Remote Sens. Environ. 150, 132–139.
Lee, S.W., Baek, S.H., Ahn, S.Y., Na, K.Y., Chae, D.-W., Chin, H.J., et al., 2016. The effects of pre-existing hyponatremia and subsequent-developing acute kidney injury on in-hospital mortality: a retrospective cohort study. PLoS One 11 (9), e0162990.
Lindstrom, S.J., Nagalingam, V., Newnham, H.H., 2013. Impact of the 2009 Melbourne heatwave on a major public hospital. Intern. Med. J. 43 (11), 1246–1250.
Lipman, G.S., Burns, P., Phillips, C., Jensen, J., Little, C., Jurkiewicz, C., et al., 2021. Effect of sodium supplements and climate on dysnatremia during ultramarathon running. Clin. J. Sport Med. 31 (6) e327-e334.
Liu, J., Varghese, B.M., Hansen, A., Borg, M.A., Zhang, Y., Driscoll, T., et al., 2021. Hot weather as a risk factor for kidney disease outcomes: A systematic review and meta-analysis of epidemiological evidence. Sci. Total Environ. 801, 149806.
Lombardi, G., Ferraro, P.M., Naticchia, A., Gambaro, G., 2021. Serum sodium variability and acute kidney injury: a retrospective observational cohort study on a hospitalized population. Intern. Emerg. Med. 16 (3), 617–624.
Lu, Y., Zeger, S.L., 2007. On the equivalence of case-crossover and time series methods in environmental epidemiology. Biostatistics 8 (2), 337–344.
Malig, B.J., Guirguis, K., Gershunov, A., Basu, R., 2019. Associations between ambient temperature and hepatobiliary and renal hospitalizations in California, 1999 to 2009. Environ. Res. 177, 108566.
Mangoni, A.A., Kholmurodova, F., Mayner, L., Hakendorf, P., Woodman, R.J., 2017. The concomitant use of diuretics, non-steroidal anti-inflammatory drugs, and angiotensin-converting enzyme inhibitors or angiotensin receptor blockers (Triple Whammy), extreme heat, and in-hospital acute kidney injury in older medical patients. Adv. Ther. 34 (11), 2534–2541.
McCullough, P.A., 2010. Prevention of cardiorenal syndromes. Cardiorenal Syndromes Crit. Care 165, 101–111.
McTavish, R.K., Richard, L., McArthur, E., Shariff, S.Z., Acedillo, R., Parikh, C.R., et al., 2018. Association between high environmental heat and risk of acute kidney injury among older adults in a northern climate: a matched case-control study. Am. J. Kidney Dis. 71 (2), 200–208.
Mendez-Lazaro, P.A., Perez-Cardona, C.M., Rodriguez, E., Martinez, O., Taboas, M., Bocanegra, A., et al., 2018. Climate change, heat, and mortality in the tropical urban area of San Juan, Puerto Rico. Int. J. Biometeorol. 62 (5), 699–707.
Munoz Sabater, J., 2019. ERA5-Land hourly data from 1981 to present. In: Copernicus Climate Change Service (C3S) Climate Data Store (CDS), editor.
NASA/METI/AIST/Japan Spacesystems and U.S./Japan ASTER Science Team. ASTER Global Digital Elevation Model V003. In: DAAC NELP, editor. 2019.
Ordon, M., Welk, B., Li, Q., Wang, J., Lavigne, E., Yagouti, A., et al., 2016. Ambient temperature and the risk of renal colic: a population-based study of the impact of demographics and comorbidity. J. Endourol. 30 (10), 1138–1143.
Ostro, B., Rauch, S., Green, R., Malig, B., Basu, R., 2010. The effects of temperature and use of air conditioning on hospitalizations. Am. J. Epidemiol. 172 (9), 1053–1061.
Reid, C.E., Mann, J.K., Alfasso, R., English, P.B., King, G.C., Lincoln, R.A., et al., 2012. Evaluation of a heat vulnerability index on abnormally hot days: an environmental public health tracking study. Environ. Health Perspect. 120 (5), 715–720.
Roncal-Jimenez, C., García-Trabanino, R., Barregard, L., Lanaspa, M.A., Wesseling, C., Harra, T., et al., 2016. Heat stress nephropathy from exercise-induced uric acid crystalluria: a perspective on Mesoamerican nephropathy. Am. J. Kidney Dis. 67 (1), 20–30.
Ross, M.E., Vicedo-Cabrera, A.M., Kopp, R.E., Song, L., Goldfarb, D.S., Pulido, J., et al., 2018. Assessment of the combination of temperature and relative humidity on kidney stone presentations. Environ. Res. 162, 97–105.
Sherbakov, T., Malig, B., Guirguis, K., Gershunov, A., Basu, R., 2018. Ambient temperature and added heat wave effects on hospitalizations in California from 1999 to 2009. Environ. Res. 160, 83–90.
Singh, P., Harris, P.C., Sas, D.J., Lieske, J.C., 2021. The genetics of kidney stone disease and nephrocalcinosis. Nat. Rev. Nephrol. 1–17.
Tasian, G.E., Pulido, J.E., Antonio, G., Saigal, C.S., Horton, B.P., Richard, J.L., et al., 2014. Daily mean temperature and clinical kidney stone presentation in five U.S. metropolitan areas: a time-series analysis. Environ. Health Perspect. 122 (10), 1081.
WMO_Geneva. Guide to meteorological instruments and methods of observation (WMO-No. 8). 2018.
US Department of Health Human Services CfDCP. Chronic kidney disease in the United States, 2021 Atlanta, GA2021 [3]. Available from: https://www.cdc.gov/kidneydisease/pdf/Chronic-Kidney-Disease-in-the-US-2021-h.pdf.
Vaneckova, P., Bambrick, H., 2013. Cause-specific hospital admissions on hot days in Sydney. Australia. PLoS One. 8 (2).
Vicedo-Cabrera, A.M., Goldfarb, D.S., Kopp, R.E., Song, L., Tasian, G.E., 2020. Sex differences in the temperature dependence of kidney stone presentations: a population-based aggregated case-crossover study. Urolithiasis. 48 (1), 37–46.
Vose, R.S., Applequist, S., Squires, M., Durre, I., Menne, M.J., Williams Jr, C.N., et al., 2014. Improved historical temperature and precipitation time series for US climate divisions. J. Appl. Meteorol. Climatol. 53 (5), 1232–1251.
Wan, Z., Hook, S., Hulley, G., 2015. MOD11A1 MODIS/Terra Land Surface Temperature/Emissivity Daily L3 Global 1km SIN Grid V006. In: NASA EOSDIS Land Processes DAAC, editor.
Wang, Y.C., Lin, Y.K., 2014. Association between temperature and emergency room visits for cardiorespiratory diseases, metabolic syndrome-related diseases, and accidents in metropolitan Taipei. PLoS One 9 (6), e99599.
Wilson, L.A., Morgan, G.G., Hanigan, I.C., Johnston, F.H., Abu-Rayya, H., Broome, R., et al., 2013. The impact of heat on mortality and morbidity in the Greater Metropolitan Sydney Region: a case crossover analysis. Environ. Health 12, 98.
Wu, C.Y., Zaitchik, B.F., Swarup, S., Gohlke, J.M., 2019. Influence of the spatial resolution of the exposure estimate in determining the association between heat waves and adverse health outcomes. Ann. Am. Assoc. Geogr. 109 (3), 875–886.

Xia, Y., et al., 2009. NCEP/EMC. NLDAS Primary Forcing Data L4 Hourly 0.125 x 0.125 degree V002, Edited by David Mocko, NASA/GSFC/HSL, Greenbelt, Maryland, USA, Goddard Earth Sciences Data and Information Services Center (GES DISC).
Xia, Y., Mitchell, K., Ek, M., Sheffield, J., Cosgrove, B., Wood, E., et al., 2012. Continental-scale water and energy flux analysis and validation for the North American Land Data Assimilation System project phase 2 (NLDAS-2): 1. Intercomparison and application of model products. J. Geophys. Res.: Atmos., 117, D3.
Yang, C., Chen, X., Chen, R., Cai, J., Meng, X., Wan, Y., et al., 2015. Daily ambient temperature and renal colic incidence in Guangzhou, China: a time-series analysis. Int. J. Biometeorol. 60 (8), 1–8.
Yang, H.-C., Zuo, Y., Fogo, A.B., 2010. Models of chronic kidney disease. Drug Discov. Today Dis. Model. 7 (1–2), 13–19.
Ye, X., Wolff, R., Yu, W., Vaneckova, P., Pan, X., Tong, S., 2012. Ambient temperature and morbidity: a review of epidemiological evidence. Environ. Health Perspect. 120 (1), 19–28.